Simulation on wellbore integrity at casing shoe during fracturing for shale gas wells

Xueli Guo[1, *], *Yongjin* Yu[1], *Hongfei* Ji[1], *Jiyun* Shen[1], *Jun* LI[2], and *Bing* Li[3]

[1] CNPC Engineering Technology R&D Company Limited, Beijing, China
[2] China University of Petroleum, Beijing, China
[3] China Petroleum Logging Co., LTD, Beijing, China

Abstract. Wellbore integrity is significant to maintain and improve the production performances of shale wells. In Duvernay Canada, casing deformation near the top of Ireton with a few natural faults and cracks is severe during multi-fracturing. It is urgent to reveal the mechanism to reduce the risk of wellbore failure. In this paper, casing deformation and micro-seismic signal at casing shoe is analysed. The maximum deformation of the casing can reach to be 44.4mm. Based on the focal mechanism, it is easy to get the formation slip displacement. Under the condition of geology and wellbore geometry, a three-dimensional stage finite element method considering the whole drilling process is established to simulate the influence of fault on casing deformation. The results indicate that cement sheath at casing shoes intend to be failure during fracturing, where the fracturing fluid will immerse into the formation of Ireton thorough the micro-annulus of cement sheath. When the pore pressure is large enough to activate the natural fault, the micro-seismic signal at the casing shoe is frequent with the magnitude up to 3. Under this condition, the faults slippage can be 55 mm, and the casing deformation will be 34.9 mm. This is consistent with the actual deformation of casing. Along easy-slip formation position, cement property and wellbore structure should be optimized to prevent fracturing fluid entering the formation. Fracturing operation should be optimized to avoid generating high-magnitude seismic signals during the fracturing process, thereby reducing the possibility of casing shear deformation.

Keywords: Casing deformation, Fault slippage, FEM, Fracturing, Shale gas.

1 Introduction

In Canada, the target layer of Duvernay at south Simonette is located between 3800-4000m, and the effective reservoir thickness is 30-45 meters[1]. Volume fracturing technology can effectively improve the efficiency of reservoir. The maximum of perforations stages per well can be 42. Average mean pressures, pumping rates, and total pumped fluid volume in well for individual stages are 62.6 MPa, 9.4 m^3/min, and 1200 m^3.[2] However,

[*] Corresponding author: guoxldr@cnpc.com.cn

during the multi-stage fracturing process, the fracturing fluid is injected into the formation with high pressure and large pump rate, which makes the wellbore downhole environment extremely complicated. The high pressure and drastic temperature changes will increase the risk of casing deformation. Some researchers hold the point that multi-stage hydraulic fracturing stimulation may trigger significant variation of the in-situ stress during fracturing [3]. With the changes of stress and pressure in faults, the fault will slip and induce seismicity [4]. When the pore pressure is large enough to activate the fault to move, casing deformation will occur [5].

The casing deformation during multi-fracturing at Duvernay is severe and the mechanism need to be studied. Based on the focal mechanism, it is easy to get the formation slip displacement. A new three-dimensional stage finite element method considering the whole drilling process is established to simulate the influence of fault on casing deformation. The results are compared with the casing deformation data to verify the accuracy of the new model. Some countermeasures to prevent casing deformation are proposed to reduce the risk of wellbore integrity during fracturing for shale wells.

2 Casing deformation analysis

2.1 Casing deformation at Ireton

Casing integrity is significant to maintain and improve the production performances of shale wells. It affects the longevity of wells and the economic benefit of shale field. For a shale gas well pad in Duvernay, there were 14 casing deformation points along Ireton, including 7 severe deformation points at the top of Ireton, like the red stars shown in Figure 1. It can be seen that the maximum deformation of the casing can be 44.4mm. As a result, normal fracturing operation is greatly affected.

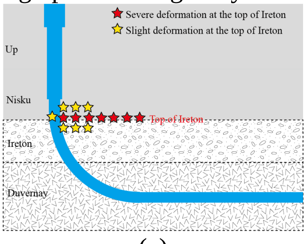

(a)

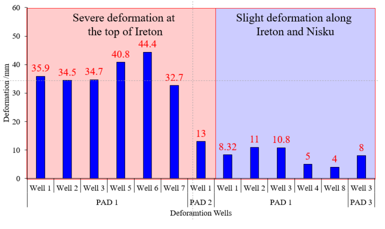

(b)

Fig. 1. Casing deformation at the top of Ireton during fracturing operation.

2.2 Micro-seismic signals analysis

Volume of fracturing fluid for shale gas well in Duvernay is always at a large scale, shown in **Figure.2** (a). It can be seen that total fluid volume injected into a well is larger than 40,000 m^3. R. Schultz et al. [6] found a sharp increase in the frequency of earthquakes in response to hydraulic fracturing. Injection pressure and rate had an insignificant association with seismic response, shown in **Figure 2** (b). Due to the complex geological conditions in this area, fractures and faults are widely distributed, it is easy to activate the faults or fractures, which brings great challenges to casing safety.

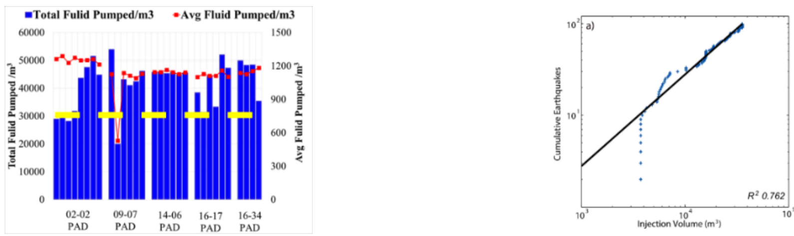

(a) (b)

Fig. 2. Seismic signals during hydraulic fracturing:(a)Fracturing fluid volume,(b)relationship between the injection fluid and seismic response.

2.3 Formation slippage distance

Casing deformation occurs at the top of Ireton. From the logging curve, in Figure 3(a), the gamma changes a lot, which means the formation is easy to slip. When it happens, the accumulated strains of the faults suddenly release with the stress drop and strong seismic signals. In general, a circular fault [7] can be used to describe micro-seismic events as shown in Figure. 3(b).

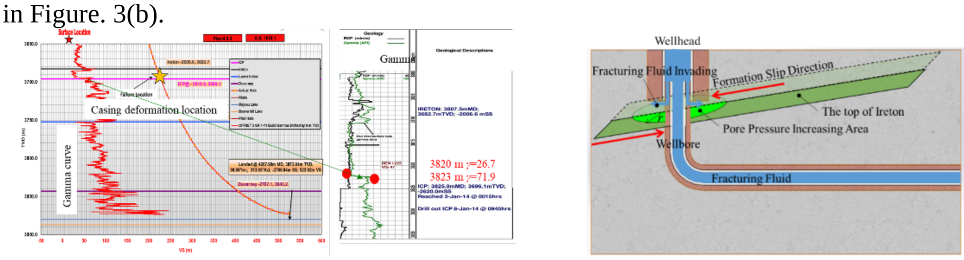

(a) (b)

Fig. 3. Logging curve and fault slip model.

The fault slip distance can be calculated by the following equations, if the fault shear modulus, strain energy release, stress drop, source dimension and moment, and radiated seismic energy.

$$r = \sqrt[3]{7\pi\rho_0 v_0^3 R\Omega_0 / (4F_c \Delta\sigma)}\ , \tag{1}$$

$$L = 16\Delta\sigma r / (7\pi G)\ , \tag{2}$$

where r is the circular fault radius (m), ρ_0 is the formation density (kg/m^3), v_0 is the wave velocity (m/s), R is the distance from the source to the detector (m), Ω_0 is the lowest frequency level of displacement (m·s), F_c is the radiation field coefficient [8], $\Delta\sigma$ is the stress drop (MPa), L is the slip distance (m), G is the formation shear modulus (MPa).

3 Finite Element Model (FEM) establishment

3.1 Stage finite element model

Under the condition of geology and wellbore geometry, a three-dimensional stage finite element method considering the whole drilling process is established to simulate the influence of fault on casing deformation. The stage FEM procedure is shown in Figure. 4.

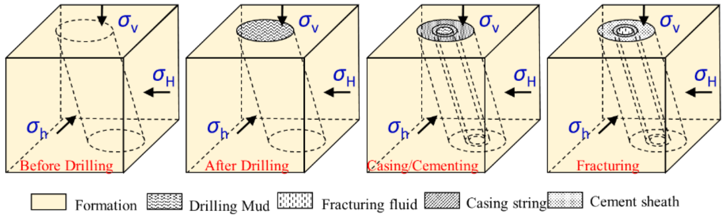

Fig. 4. Stage FEM (σ_V, σ_H, σ_h are represented the vertical stress, the maximum horizontal stress and the minimum horizontal stress, respectively).

The CCF models are developed using the 3D stress function of finite element software described above, shown in Figure. 5. The fault slip is set by changing the boundary displacements. According to the Saint-Venant principle, a formation boundary dimension should be five to six times larger than that of the well-bore geometry to avoid the influence of boundary effect on wellbore stress [9].

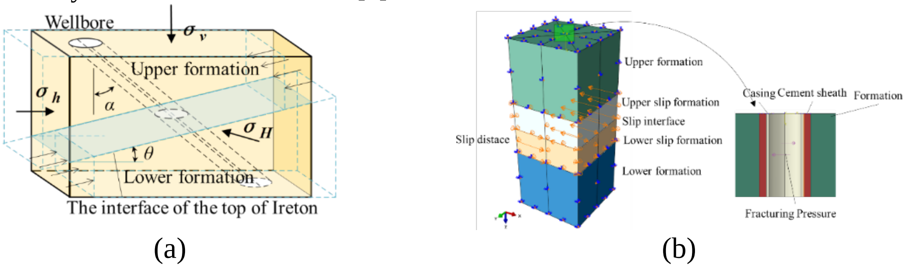

Fig. 5. FEM model at the condition of fault slippage.

Casing deformation can be obtained quantitatively by the well diameter measurement tool. The diameter of the casing after deformation can be calculated by the following formula, shown in Eq. (3),

$$D_i = 2(R_{0i} + S_i) \tag{3}$$

Where R_{0i} is the original radius of the casing at the measuring point, S_i is the deformation of the casing relative to the original position, which is the measured value of the well diameter, and R_i is the casing deformation. After the radius, D_i is the diameter of the casing after deformation.

3.2 Parameter setting

The well depth was 3774.6 m, the corresponding vertical depth was 3748 m, and the inclination angle was 31.58°. Casing steel grade was P110-ICY, the yield value was 758 MPa, the internal compressive strength was 83.4 MPa, and external extrusion strength was 99 MPa. The vertical in-situ stress, the maximum horizontal principal stress and the minimum horizontal principal stress could be set to 92.4 MPa, 85 MPa and 70.2 MPa, respectively. The internal pressure of the casing was equal to the sum of the ground pump pressure and the liquid column pressure, and then reduced to remove the friction. The result was 117.48 MPa. Other parameters are shown in Table 1.

Table 1. Parameters of FEM model.

Name	Value	Name	Value
Wellbore diameter/mm	155.58	Hydrostatic column pressure /MPa	36.95

 https://doi.org/10.1051/itmconf/20224501046

Casing diameter/mm	114.3	String friction/MPa	10
Casing inner diameter/mm	101.6	Geothermal gradient /℃/m	0.036
Boundary diameter/mm	3000	Pump rate q /m^3/min	10
G_H /KPa/m	23	Consistency coefficient $K/Pa{\cdot}s^{-n}$	0.05
G_h /KPa/m	19	Fluidity index n/s^n	0.1
G_v /KPa	25	Fracturing fluid temperature/℃	20
Pump pressure/MPa	80	Vertical depth/m	3748

4 Results

4.1 Cement sheath failure

The mechanical behaviour of casing deformation at the interface is analysed for shale gas wells which the wellbore structure is shown in Figure. 6(a). The micro-seismic signal monitored during the fracturing process is shown in Figure. 6 (b). The production casing of this well is lowered into the bottom of the well through the casing hanger, and the intermediate casing is lowered to the vicinity of the top of Ireton. The distance *L* between the casing shoes and the top of Ireton is only about 10 m. Production casing is hanged by the liner hanger above the top of Ireton, which is about 150-180 m from the interface. It can be seen that a large magnitude seismic signal appeared around the well during the fracturing process. In addition, during fracturing, not only more micro-seismic signals appeared in the fractured section, but also more micro-seismic signals appeared in the Ireton top of the non-fracturing section (shown in the red circle on the right of the figure). It means that the fracturing fluid emerges to the top of Ireton. The micro-seismic signals of magnitude 2.3 was monitored in well during the 19th fracturing section. The signal distribution is similar to that of the above well, indicating that the formation slipped at the top of Ireton

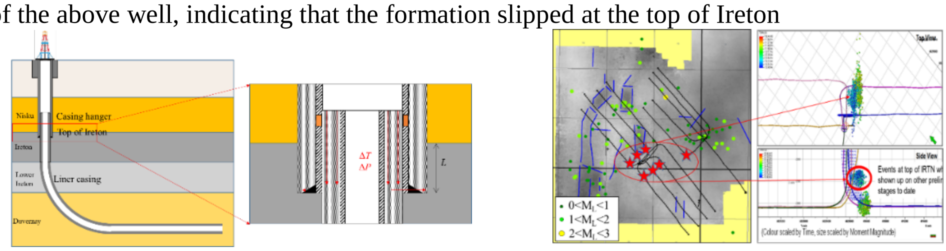

(a) (b)

Fig. 6. Well structure and micro-seismic during fracturing: (a) L is presented the distance between the casing shoes and the top of Ireton, (b) Micro-seismic distribution characteristics

In the process of multi-stage fracturing, it will experience up to 40 alternating changes for temperature and pressure, and the cement sheath will withstand severe load fluctuation. From the numerical simulation, shown in Figure. 7, the circumferential stress of the cement sheath produces a sudden change of tension and compression at the interface. The upper part is tensile stress and the lower part is compressive stress. The cement sheath is prone to be tensile failure, resulting in cracks. Then the fracturing fluid will enter through these channels to the top of Ireton.

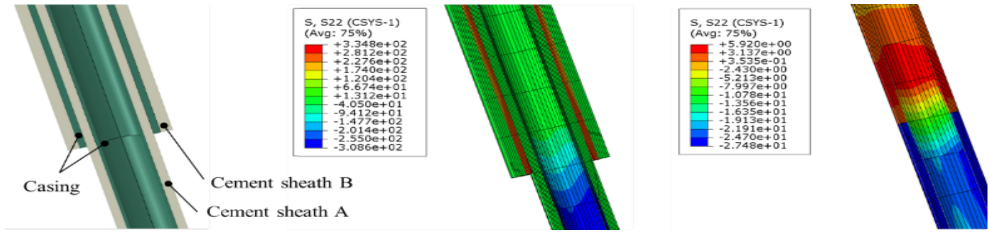

Fig. 7. Cement sheath failure analysis: (a) casing-cement sheath-formation (CCF) assembly (b) stress cloud diagram of CCF (c) stress cloud diagram of cement sheath A..

4.2 Casing deformation

The slipping displacement *L* was 55 mm when the micro-seismic occurred with the degree of M3.0, which is substituted into the finite element model to calculate the casing deformation. The finite element model result is shown in Figure. 8. It can be seen from the figure that the casing deformation shape was similar to the well diameter shape measured with multi-finger calliper. It indicates that the casing displacement have a sudden change at the sliding interface, and the maximum deformation can reach 34.9 mm. The deformation of the casing measured by the tool was 32.7 mm which is similar to the simulation result.

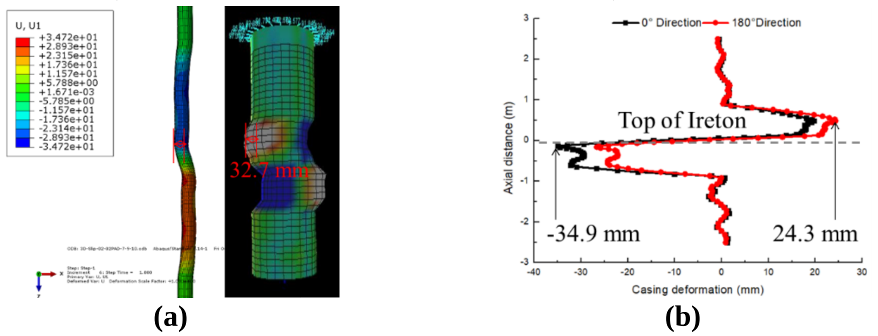

Fig. 8. Comparison of finite element results and calliper measurement: (a) Comparison of finite element and borehole diameter measurement (b) Axial deformation of finite element.

The diameter of the deformed casing can be calculated using Eq. 4, and the comparison between the actual casing diameter measured and simulation result is shown in Figure. 9. It can be seen that the casing deformation shape simulated by finite element model is similar to the actual measured, indicating that the casing deformation is mainly caused by the sheath slip of fault.

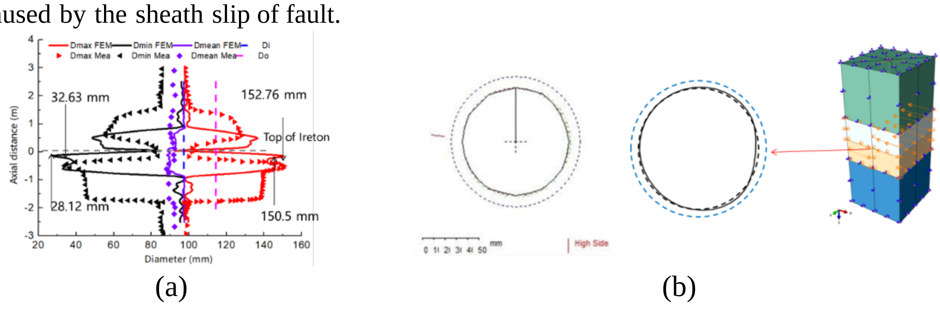

Fig. 9. Casing axial deformation comparison for shale gas well.

5 Conclusion

Based on the condition of geology and wellbore geometry, a three-dimensional finite element method considering the whole drilling process is established to simulate the influence of fault slippage on casing deformation. The fault slip distance can be calculated using micro-seismic data based on the source mechanism. Some conclusion can be draw. Sever casing deformations occur at the top of Ireton, where large amounts of fluid are injected into the formation and fault cracks are widely distributed. The increasing pore pressure causes the stress field changing abruptly. It can easily reactivate the formation to slip. The cement sheath will be failure with multiple alternating of pressure and temperature, causing crack in the cement sheath, then fracturing fluid enters the formation thorough the cement cracks. The maximum deformation is about 34.9 which is consisted with the value obtained with multi-finger calliper. The deformation shape of casing is similar with the actual condition. It indicates that fault slippage can shear the casing, resulting in casing deformation, accompanied by high-magnitude seismic signals. Some measures can be carried to avoid casing deformation. Near the formation with large amount natural fault or crack, cement sheath integrity is very important. Cement property and wellbore structure should be optimized to prevent cement failure to avoid fracturing fluid entering the formation. Fracturing pump rate should be optimized to avoid generating high-magnitude seismic signals during the fracturing process, thereby reducing the possibility of casing shear deformation.

This work was supported by China National Petroleum Corporation Scientific Research and Technology Development Project (Grant No. 2021DJ4403, 2020F-49).

References

1. C. Zhaowei, S. Lin, X. Degui. Mechanism of casing deformation in the Changning–Weiyuan national shale gas demonstration area and countermeasures[J]. Natural Gas Industry. 2017, 4(1): 1-6.
2. C. Sugden, J. Johnson, M. Chambers, et al. Special Considerations in the Design Optimization of High Rate, Multistage Fractured Shale Wells[C]. IADC/SPE Drilling Conference and Exhibition, 2012.
3. Z. Moradian, A. Fathi, B. Evans. Shear Reactivation of Natural Fractures in Hydraulic Fracturing[C]. American Rock Mechanics Association, 2016.
4. S.P. Lele, T. Tyrrell, G.R. Dasari. Geomechanical Analysis of Fault Reactivation Due to Hydraulic Fracturing[C]. American Rock Mechanics Association, 2017.
5. G. Xueli, L. Jun, L. Gonghui, et al. Numerical simulation of casing deformation during volume fracturing of horizontal shale gas wells[J]. Journal of Petroleum Science and Engineering. 2019, 172: 731-742.
6. R. Schultz, G. Atkinson, D.W. Eaton, et al. Hydraulic fracturing volume is associated with induced earthquake productivity in the Duvernay play[J]. Science, 2018, 359(6373): 304-308.
7. C. Cipolla, S. Maxwell, M. Mack, et al. A Practical Guide to Interpreting Microseismic Measurements[C]. SPE 144067, 2011.
8. R.E. Goodman. Introduction to Rock Mechanics[M]. Canada: Wiley, 1989.
9. K.E. Gray, E. Podnos, E. Becker. Finite-Element Studies of Near-Wellbore Region During Cementing Operations: Part I[J]. SPE Drill & Completion. 2009, 24(01): 127-136.